Supercontinuum generation at 1.55 μm in an all-normal dispersion photonic crystal fiber with high-repetition-rate picosecond pulses*

XU Yong-zhao (徐永钊)[1]**, **HAN Tao** (韩涛)[1], **SONG Jian-xun** (宋建勋)[1,2], **LING Dong-xiong** (凌东雄)[1], **and LI Hong-tao** (李洪涛)[1]

1. School of Electronic Engineering, Dongguan University of Technology, Dongguan 523808, China

2. Institute of Dongguan-Sun Yat-Sen University, Dongguan 523808, China

(Received 28 August 2014)

We demonstrate the generation of supercontinuum (SC) spectrum covering S+C+L band of optical communication by injecting 1.4 ps optical pulses with center wavelength of 1 552 nm and repetition rate of 10 GHz into an all-normal dispersion photonic crystal fiber (PCF) with length of 80 m. The experimental results are in good agreement with the numerical simulations, which are used to illustrate the SC generation dynamics by self-phase modulation and optical wave breaking (WB).

Document code: A **Article ID:** 1673-1905(2014)06-0463-4

DOI 10.1007/s11801-014-4153-0

Photonic crystal fibers (PCFs) are micro-structured optical fibers which offer the flexibilities of dispersive and nonlinear properties and have been extensively used for supercontinuum (SC) generation, telecommunication, high power transmission and optical sensing[1-6]. Broadband light sources based on SC generation at telecom-band have important application in the wavelength division multiplexing (WDM) optical transmission system and radio over fiber (ROF) system[5,6].

SC spectra are usually generated by pumping PCF with femtosecond or picosecond pulses in the anomalous dispersion regime of the PCF close to the zero dispersion wavelength (ZDW)[1]. The broadening mechanism in this case is dominated by soliton dynamics, which is sensitive to input pulse fluctuations, resulting in large differences in spectral structure from pulse to pulse[1,7,8]. Consequently, these ultra-broad SCs are characterized by a complex temporal profile, pulse to pulse variations in intensity and phase, as well as considerable fine structures over their bandwidth[9,10]. In many applications, low noise and high stability are the essential characteristics of the SC. In order to reduce this noise, soliton effects and the associated problems must be avoided. It can be realized by generating the SC entirely in the normal dispersion regime where the spectral broadening is mainly through self-phase modulation (SPM). Therefore, SC generation in the normal dispersion regime is expected to produce spectra with high coherence and stability[11,12].

In this paper, SC generation in an all-normal dispersion PCF (ANDi PCF) with high-repetition-rate picosecond pulses is demonstrated. An SC spectrum covering S-, C- and L-bands of optical communication and spanning from 1 445 nm to almost 1 640 nm is generated. Numerical simulations are also used to illustrate the SC generation dynamics by SPM and optical wave breaking (WB).

The schematic diagram of experimental setup is shown in Fig.1. A passively mode-locked semiconductor laser is used as pump source, which can generate 1.4 ps and $sech^2$-shaped short pulses. The laser output pulses are centered at 1 552 nm with average power of 0.26 mW at a repetition rate of 10 GHz. After passing through a polarization controller (PC), the pulses are amplified with an erbium-doped fiber amplifier (EDFA) and coupled into the PCF. The pulses coming out of the PCF are attenuated using a variable optical attenuator (VOA) and fed into an optical spectrum analyser (OSA) for analysis.

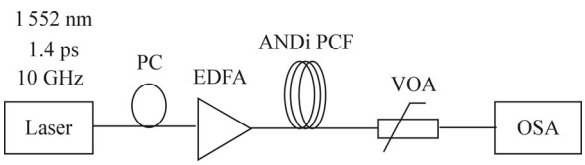

Fig.1 Schematic diagram of the experimental setup

In this paper, we use an 80 m-long ANDi PCF for SC generation. The fiber supplied by NKT Photonics (Denmark) has a three-fold symmetric hybrid core region with

* This work has been supported by the Guangdong Science and Technology Program (No.2012B090600009), and the Guangdong Natural Science Fund (No.10451170003004948).

** E-mail: yongzhaoxu@126.com

core diameter of 2.1 μm, and achieves the nonlinear coefficient of ~11 $W^{-1}\cdot km^{-1}$. The cross section of the fiber is shown in the inset of Fig.2. The dispersion curve of the fiber is also shown in Fig.2. It indicates that the PCF does not possess any ZDW and exhibits a convex dispersion profile which solely covers the normal dispersion region. The dispersion coefficient of the fiber is about –0.55 ps/(nm·km) at 1 552 nm, and the dispersion variation is less than 1.5 ps/(nm·km) between 1 500 nm and 1 650 nm.

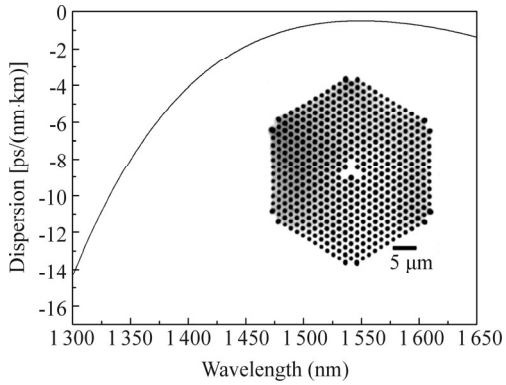

Fig.2 Dispersion curve and cross-section image of the ANDi PCF used in the experiment

In our experiments, we find that the output spectrum depends on the input polarization state, so we adjust the polarization controller to obtain the broadest spectrum. Fig.3 shows the typical measured spectra for various pump power. The average coupling powers into the fiber are 0.59 W, 1.03 W and 1.88 W, respectively. In order to better observe the evolution of spectra, we show the spectra in linear scale. Note that the spectral broadening is proportional to the input power, and a higher input power brings a broader spectrum. The most notable feature of the generated spectra is that the spectral broadening is accompanied by an oscillatory structure covering the spectrum range. Those features show a typical pattern of SPM-induced spectral broadening. The multipeak structure in the spectrum is created by the spectral interference of identical spectral components located at different temporal positions within the pulse.

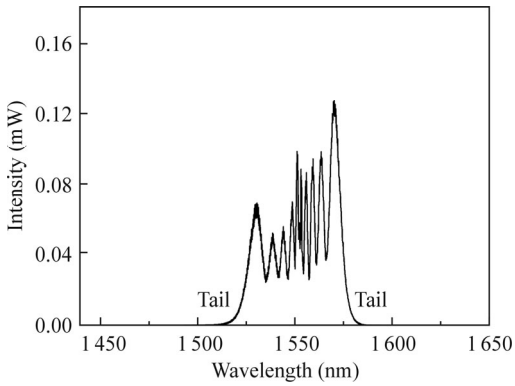

(a) 0.59 W

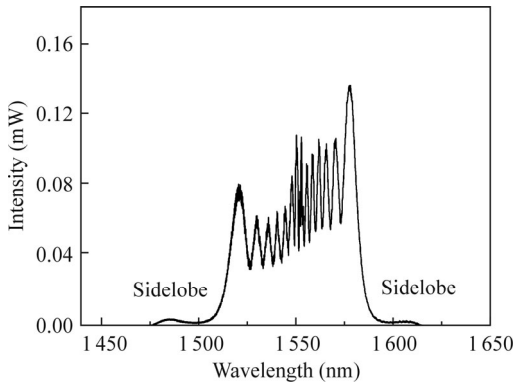

(b) 1.03 W

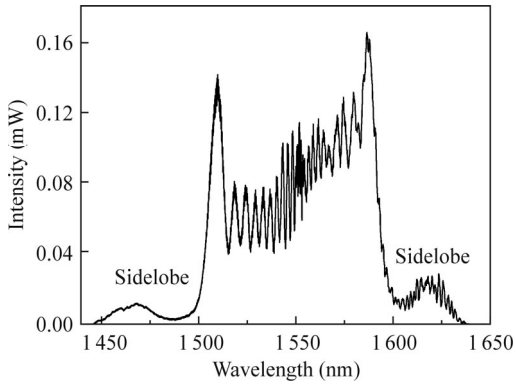

(c) 1.88 W

Fig.3 Experimental SC spectra generated from the ANDi PCF with average coupling powers of (a) 0.59 W, (b) 1.03 W and (c) 1.88 W

Interestingly, at the lowest power, long tails emerge from the pulse spectrum at both short and long wavelength ends of the characteristic SPM fringes as shown in Fig.3(a). At the intermediate power, the tails develop into two well-defined sidelobes on either side of the SPM-extended spectrum region as shown in Fig.3(b). These spectral changes at both edges of the SPM fringes strongly suggest the occurrence of WB. At the highest power as shown in Fig.3(c), WB fully develops and the spectral extension of WB is maximized. It can be seen from Fig.3(c) that the SC spectrum spans from 1 445 nm to almost 1 640 nm which covers S-, C- and L-bands of optical communication. Because the pump wavelength deviates from the wavelength corresponding to the maximum of the dispersion curve, the broadening occurs asymmetrically.

From the experimental results, we also note that at relatively low input power, the spectral broadening is dominated by SPM. Therefore, the achievable bandwidth of the spectrum solely depends on the amount of SPM-induced broadening. If the input power exceeds the WB limit, the spectral edges of the SPM-extended SC are further extended by WB.

Furthermore, we numerically simulate the SC generation in the ANDi PCF by solving the nonlinear Schrödinger equation using the split-step Fourier method[13]. The simu-

lated spectra and pulses output from the fiber at the three coupling powers used in the experiments are shown in Figs.4 and 5. The simulated spectra shown in Fig.4(a)–(c) are found to be in good agreement with the observed spectra shown in Fig.3(a)–(c). The origin of these tails or sidelobes can be clarified if the simulated SC pulses are presented in the time domain as shown in Fig.5(a)–(c). At the lowest coupling power of 0.59 W, the edges of the pulse experience pronounced steepening effect. This effect precedes WB, which is evidenced by the temporal oscillations immediately following the leading and trailing edges of the pulse.

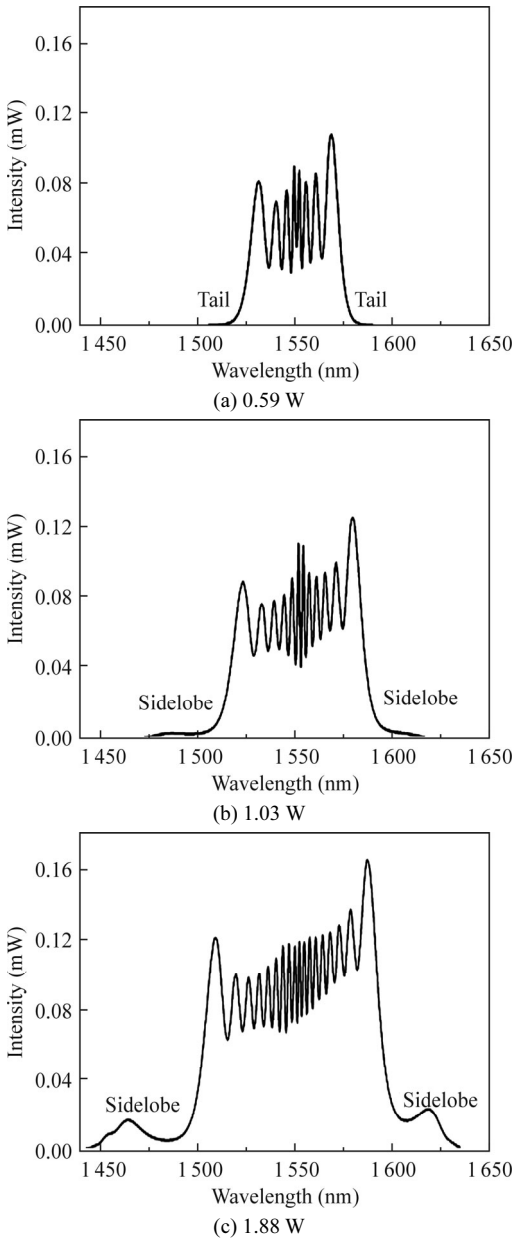

Fig.4 Theoretical SC spectra from the ANDi PCF at three coupling powers of (a) 0.59 W, (b) 1.03 W and (c) 1.88 W

These oscillations reflect the interference between two different frequency components of the pulse, which leads to the tails in the pulse spectrum through four-wave mixing (FWM)[13-15]. At elevated coupling power, the oscillations following the leading and trailing edges strengthen so that the tails develop into intense sidelobes. The simultaneous appearance of the temporal oscillations and spectral tail corresponding to either the trailing or leading pulse edge unambiguously confirms the occurrence of WB and the WB origin of the spectral tails or sidelobes. Temporal oscillations near pulse edges and the

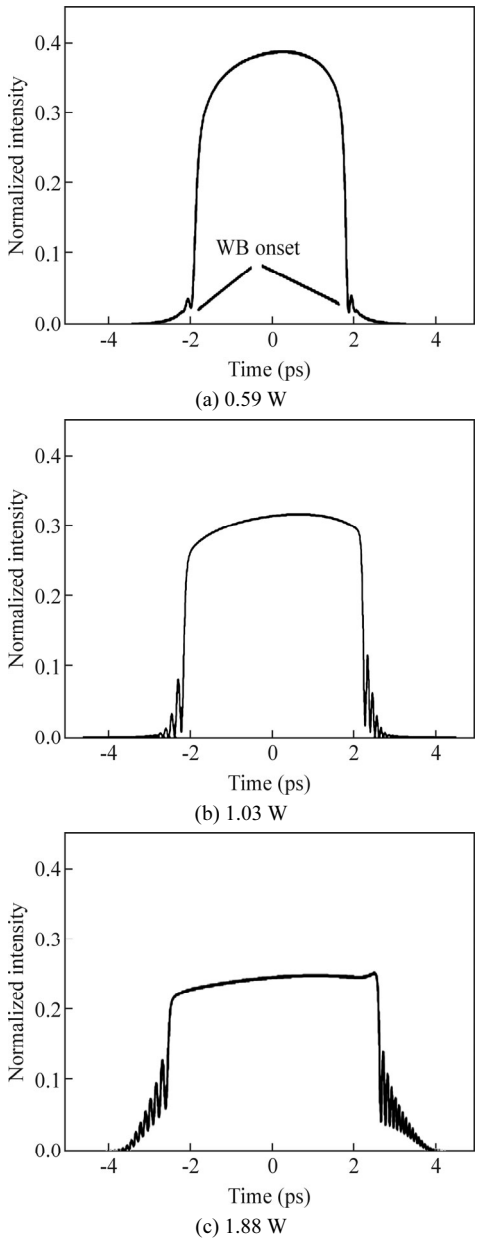

Fig.5 Theoretical pulse profiles in time domain at three coupling powers of (a) 0.59 W, (b) 1.03 W and (c) 1.88 W

pectral sidelobes are the manifestations of the same phenomenon. WB-induced FWM processes are not phase-matched. Therefore, the achievable bandwidth of the spectrum depends on the amount of SPM-induced broadening before WB occurs. The wider the separation

between SPM-generated components and the original center wavelength of the pulse at the point of WB, the broader the spectrum will be. Therefore, flat dispersion slopes, higher pump power or higher nonlinearity can enhance the spectral broadening.

In summary, we demonstrate the broadband SC generation in 1.55 μm region by picosecond pulses propagating in an 80 m-long ANDi PCF. An SC spectrum over the wavelength range from 1 445 nm to 1 640 nm is achieved. Furthermore, we perform the nonlinear Schrödinger equation based simulation to illustrate the SC generation dynamics. The experimental results are found to be in good agreement with the numerical simulations. The SC generation process in ANDi PCF is dominated by SPM and WB. If the SC is generated beyond the WB limit by using a higher input power, the spectral edges of the SPM-extended SC are further extended by WB.

References

[1] J. M. Dudley, G. Genty and S. Coen, Review of Modern Physics **78**, 1135 (2006).

[2] S. V. Smirnov, J. D. Ania-Castanon, T. J. Ellingham, S. Kobtsev and S. K. Turitsyn, Optical Fiber Technology **12**, 122 (2006).

[3] Lijia Zhang, Xiangjun Xin, Bo Liu, Yongjun Wang, Jianjun Yu and Chongxiu Yu, Optics Express **18**, 15003 (2010).

[4] GAO Lei, HOU Zhi-yun, ZHOU Gui-yao, XIA Chang-ming, CHEN Yan and TIAN Yun-yun, Journal of Optoelectronics·Laser **25**, 887 (2014). (in Chinese)

[5] HAN Ting-ting, LIU Yan-ge and WANG Zhi, Journal of Optoelectronics·Laser **23**, 215 (2012). (in Chinese)

[6] LANG Wen-yong, DAI Bing and TANG Dong-Lin, Journal of Optoelectronics·Laser **24**, 1268 (2013). (in Chinese)

[7] M. N. Islam, G. Sucha, I. Bar-Joseph, M. Wegener, J. P. Gordon and D. S. Chemla, Journal of the Optical Society of America B **6** , 1149 (1989).

[8] J. Herrmann, U. Griebner, N. Zhavoronkov, A. Husakou, D. Nickel, J. C. Knight, W. J. Wadsworth, P. St. J. Russell and G. Korn, Physical Review Letters **88**, 1739011 (2002).

[9] K. L. Corwin, N. R. Newbury, J. M. Dudley, S. Coen, S. A. Diddams, B. R. Washburn, K. Weber and R. S. Windeler, Applied Physics B **77**, 269 (2003).

[10] J. M. Dudley and S. Coen, Optics Letters **27**, 1180 (2002).

[11] A. M. Heidt, Journal of the Optical Society of America B **27**, 550 (2010).

[12] L. E. Hooper, P. J. Mosley, A. C. Muir, W. J. Wadsworth and J. C. Knight, Optics Express **19**, 4902 (2011).

[13] G. P. Agrawal, Nonlinear Fiber Optics, 3rd ed, Academic, 2001.

[14] W. J. Tomlinson, R. H. Stolen and A. M. Johnson, Optics Letters **10**, 457 (1985).

[15] C. Finot, B. Kibler, L. Provost and S. Wabnitz, Journal of the Optical Society of America B **25**, 1938 (2008).